The GEO – Project
A Long-Baseline Laser Interferometer for the Detection of Gravitational Waves

K. Danzmann, J. Chen, P.G. Nelson, T.M. Niebauer, A. Rüdiger, R. Schilling, L. Schnupp, K.A. Strain, H. Walther, and W. Winkler

Max-Planck-Institut für Quantenoptik, D-8046 Garching, Germany

J. Hough, A.M. Campbell, C.A. Cantley, J.E. Logan, B.J. Meers, E. Morrison, G.P. Newton, D.I. Robertson, N.A. Robertson, S. Rowan, K.D. Skeldon, P.J. Veitch, and H. Ward

Department of Physics, University of Glasgow, Glasgow, UK

H. Welling, P. Aufmuth, I. Kröpke and D. Ristau

Laser-Zentrum and Institut für Quantenoptik, Universität Hannover, D-3000 Hannover, Germany

J.E. Hall, J.R.J. Bennett, I.F. Corbett, B.W.H. Edwards, R.J. Elsey, and R.J.S. Greenhalgh

Rutherford Appleton Laboratory, Chilton, Didcot, UK

B.F. Schutz, D. Nicholson, and J.R. Shuttleworth

Department of Physics, University of Wales, Cardiff, UK

J. Ehlers, P. Kafka, and G. Schäfer

Max-Planck-Institut für Astrophysik, D-8046 Garching, Germany

H. Braun

Bauabteilung der Max-Planck-Gesellschaft, D-8000 München, Germany

V. Kose

Physikalisch-Technische Bundesanstalt, D-3300 Braunschweig and D-1000 Berlin, Germany

1 Introduction

More than 70 years ago, Gravitational Waves have been predicted as one of the consequences of Einstein's Theory of General Relativity. Einstein describes gravity as a curvature of space-time [1]. When the curvature is weak, it produces Newtonian gravity that we are so familiar with. But a strong curvature behaves in a very different, non-linear fashion. Actually curvature can produce curvature without the aid of any matter. Fast variations of the curvature in time, (due to stellar collapse or collisions, for example) should produce ripples in the fabric of space-time that propagate out at the speed of light and carry the information about the underlying cosmic events. Gravitational waves are clearly one of the fundamental building blocks of our theoretical picture of the universe and there is some circumstantial evidence pointing to their existence [2]. But in spite of numerous attempts over the last 30 years, their direct detection remains as one of the great unsolved problems of experimental physics.

1.1 The Birth of Gravitational Astronomy

Today, the technology seems to be in hand to finally tackle this problem and this article is aiming at outlining the current efforts to bring non-linear gravity into confrontation with experiment through the detection of gravitational waves. But the final aim is not a mere proof of the existence of gravity waves, rather to make them useful for observational astronomy through the creation of a world-wide network of detectors. We have to realize that the information carried by gravitational waves is complementary to the information carried by electro-magnetic radiation. Whereas electro-magnetic radiation is an incoherent superposition of radiation mostly emitted by thermally excited atoms and high-energy electrons, it is the coherent, bulk motion of huge amounts of mass that produces significant levels of gravity waves. Electro-magnetic radiation is easily scattered and absorbed, but gravitational radiation is transmitted almost undisturbed through all forms and amounts of intervening matter [3]. The introduction of Gravitational Astronomy would thus literally open a new window to the universe.

Nobody really knows with certainty how hard it will be to open this window. It is difficult to predict, from our present knowledge based on electromagnetic radiation, just how sensitive a detector has to be to begin to see gravitational waves. But once it does see waves, it will give us information about the universe that we have almost no hope of gaining in any other way. Optical and radio telescopes are sensitive to stellar atmospheres, interstellar dust or primordial gas, all things that a gravitational wave detector will

not see. Instead, we will learn about the inspiral and coalescence of black hole and neutron star binaries, their birth-rates and distribution in distant galaxies, the final collapse of asymmetric supernova cores, "cosmic strings", and the first millisecond of the big bang [4].

2 The Detection of Gravitational Waves

Gravitational waves change the metric of space-time. They can be detected through the strain in space created by their passage. Consider a gravity wave impinging perpendicular to the plane of a circle, see Fig.1. During the first half-cycle of the wave, the circle will be deformed into a standing ellipse and during the second half-cycle into a horizontal ellipse. It is the fractional change in diameter that is commonly quoted as a measure for the amplitude, $h = 2dL/L$, of a gravitational wave. The principle behind the detection of gravity waves is thus a simple length measurement. The problem is that the length change is so small. As an example, consider a supernova in a not too distant galaxy. This might produce a relative length change here on earth of 1 part in 10^{21}. Such a relative length change corresponds to the diameter of one hydrogen atom on the distance from here to the sun, or equivalently to a thousandth of a proton diameter on GEO's 3 km long detector arms. And this happens during a few milliseconds only.

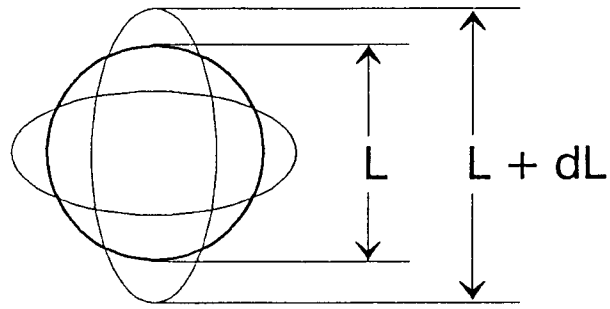

Fig. 1. Gravitational waves change distances by squeezing space.

2.1 Bar Antennas

The history of attempts to detect gravity waves began in the 1960s with the famous bar experiments of Joseph Weber [5]. Bar antennas, in principle, are very simple objects. Imagine a large cylindrical block of e.g. aluminum that during the passage of a gravitational wave gets excited similarly to being struck with a hammer. Even though these experiments have not yet

detected gravitational waves, they had the undisputed effect of alerting the scientific community to the possibility of experimentally detecting gravity waves. Bar detectors have in the meantime been developed and refined in several places all over the world. Being supercooled to mK temperatures and equipped with very sophisticated length transducers [6], they have now reached a sensitivity ($h = 10^{-18}$ for millisecond pulses) where they could expect to see the next supernova in our own galaxy, and they are likely to remain an important ingredient of the world-wide gravity wave-watch. But being resonant devices, they are in practice sensitive only in a relatively narrow band around their central frequency. They are also limited in their sensitivity through the quantum-mechanical uncertainty of their mechanical state, although this limitation may in priciple be overcome by QND techniques, and so their usefulness will in all likelihood remain very limited for the forseeable future.

2.2 Laser Interferometers

Although the seeds of the idea can already be found in early papers by Pirani [7] and Gertsenshtein and Pustovoit [8], it was really in the early 1970s when the idea emerged that laser interferometers might have a better chance of detecting gravity waves, mainly promoted by Weiss [9] and Forward [10]. Large interferometers would offer the additional advantage of having broad-band sensitivity and they would not be limited by the uncertainty principle until well below a sensitivity of 10^{-23}. A Michelson interferometer measures the phase difference between two light fields having propagated up and down two perpendicular directions, i.e. essentially the length difference between the two arms. This is exactly the quantity that would be changed by the passage of a properly oriented gravitational wave, see Fig. 2.

Immediately obvious at this point is the need for long interferometer arms. The quantity measured is the absolute phase difference between the fields. But the gravity wave induces a fractional length change. So the phase difference measured can be increased by increasing the armlength or, equivalently, the interaction time of the light with the gravity wave. This works up to an optimum for an interaction time equal to half a gravity wave period. For a gravity wave frequency of 1 kHz this corresponds to half a millisecond or an armlength of 75 kilometers.

2.2.1 Long Light-Path

While it is clearly impractical to build such a large interferometer, there are ways to increase the interaction time without increasing the physical arm-length beyond reasonable limits (see the two following contributions by W. Winkler and A. Rüdiger). Historically, two approaches have emerged: storing the light in the arms in resonant optical Fabry-Perot cavities [11] and

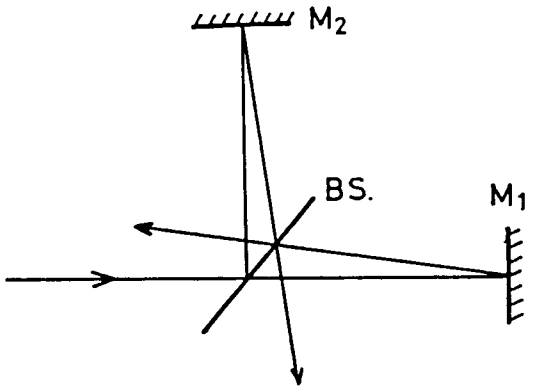

Fig. 2. Michelson interferometer

literally folding the light back and forth in optical delay lines [12]. Nowadays this distinction is beginning to disappear, because with the development of Dual Recycling [13], a new optical technique, to be discussed later, we now have a hybrid arrangement in our hands that combines the advantages of both approaches and more.

2.3 Prototypes

Several small prototypes of laser interferometric gravitational wave detectors have been developed in the world, a delay-line based interferometer with 30 m armlength at the Max-Planck-Institut für Quantenoptik in Garching, a Fabry-Perot based instrument with 10 m armlength at the University of Glasgow, a delay-line based instrument with 10 m armlength at the Institute for Space and Astronautical Science in Tokyo, and a Fabry-Perot based instrument with 40 m armlength at the California Institute of Technology. With arm-lengths on the order of a few tens of meters these prototypes are clearly too small to permit observations of real gravity waves. Their sensitivities have continually been improved over the years, and the larger ones have all reached sensitivities for millisecond pulses roughly equivalent to the best bar detectors, but in addition they are broad-band devices.

While the absolute sensitivity reached by the prototype detectors is certainly encouraging, it is much more important that they are well-understood devices. That is, the various physical processes creating noise sources at the various frequencies have to be identified in order to find ways to improve on those. In Fig. 3 we see such a noise analysis for the Garching 30-m prototype [14].

Shown is the spectral density of the apparent mirror displacement as expected from the most important noise sources. For comparison, the measured spectral density of displacement noise is also given. Very good agree-

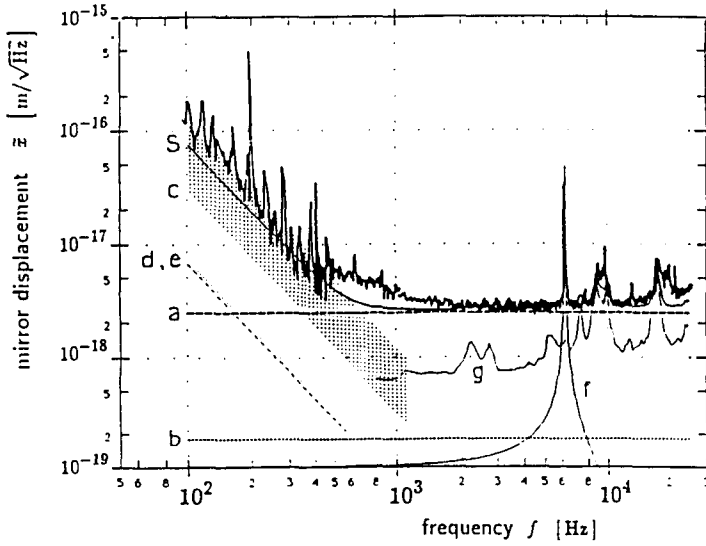

a: photon shot noise
b: residual gas fluctuations
c: filtered ground motion
d: electronic damping system
f: mirror thermal motion
e: pendulum thermal motion
g: laser frequency fluctuations

Fig. 3. Noise analysis of the Garching 30-m prototype

ment between the measured and the expected noise is found. The additional sharp peaks at frequencies of a few hundred Hertz are due to violin string resonances of the suspension wires holding the mirrors. The sensitivity of the prototype is presently limited by residual ground motion at frequencies below 1 kHz (labeled c in Fig. 3), by the photon shot noise corresponding to the available laser power at frequencies between 1 kHz and 6 kHz (labeled a), by the thermallly excited internal mechanical vibration of the mirrors in a narrow peak at 6 kHz (labeled f), and by residual frequency fluctuations of the laser at higher frequencies (labeled g). At the present level of sensitivity, the refractive index fluctuations due to the Brownian motion of the residual gas in the vacuum pipe (labeled b) are unimportant. Also unimportant at this level are the above-resonant wing of the thermally excited mirror suspension pendulum resonance (labeled e), the sub-resonant wing of the mirror internal mechanical resonance (labeled a), and the noise introduced by the electronic damping system for the mirror suspension (labeled d, see also Sect. 3.6.1).

3 The GEO Project

After almost two decades of research on small prototypes, the time had come to proceed towards the construction of full-scale interferometers with arm-lengths of several kilometers, and several such proposals were submitted at the end of the 1980s. Out of ten research groups in Germany and Britain, the GEO collaboration was formed [15], aiming at the construction of a laser interferometer with 3 km arm-length near Hannover in the German state of Niedersachsen. The research groups involved are listed at the beginning of this contribution.

In the following, the main problems encountered in the design of such an interferometer and the envisioned solutions are highlighted using the GEO project as an example. But it should be emphasized that the problems are common to all projects and that there actually is a very strong coordination and sharing of tasks between the various collaborations, especially between the German-British GEO project and the French-Italian VIRGO project. An overview of the current status (spring of 1992) of the world-wide efforts is given at the end.

3.1 The Laser Source

The sensitivity of a simple Michelson interferometer with optimized arm-length to gravitational wave bursts is limited by the photon shot noise to

$$h_{DL} \approx 2.4 \times 10^{-21} \left[\frac{\epsilon I_o}{50\,\mathrm{W}}\right]^{-1/2} \left[\frac{f}{1\,\mathrm{kHz}}\right]^{3/2}, \qquad (1)$$

where ϵ is the quantum efficiency of the detector, I_o is the laser output power, and f is the center frequency of the burst. Green light and a bandwidth of half the center frequency have been assumed. The first problem to be solved is thus the construction of a laser with sufficient output power in a stable single transverse and longitudinal mode. Moreover, frequency as well as amplitude of the laser have to be stabilized to unprecedented values.

3.1.1 Output Power

Currently all operating prototypes use Argon ion lasers as light sources. The most powerful commercially available lasers of this type offer a single-mode output power of about 5 W. The coherent addition of several such lasers phase-locked to a master oscillator to reach higher output power has been demonstrated experimentally [16]. But this approach does not seem promising because of the poor energy efficiency of these lasers (only about 10^{-4}), their complexity and high cost of operation and their poor free-running noise that requires elaborate means for stabilization. The laser source under development for the GEO detector is an all-solid state YAG laser pumped

by laser diodes. YAG lasers have traditionally been pumped by discharge lamps, but the dramatic advances in the development of laser diodes in the last few years have now made it possible to replace the noisy and inefficient lamps with diode lasers [17].

This laser will be based on a diode-pumped miniature monolithic ring laser oscillator (see Fig. 4) with an output power of a few hundred milliwatts. The oscillator incorporates an electro-optic phase modulator to permit fast tuning and easy frequency stabilization. The output of this oscillator is then amplified in diode-pumped YAG slabs enclosed in discrete ring resonators. The oscillator is operational and by the end of 1992 the final laser system is expected to deliver a single-mode output power of more than 50 W at a wavelength of 1064 nm. Although the fundamental wavelength of this laser could be used in an interferometer (and there may actually be advantages as far as the fundamental absorption in optical components is concerned) we are investigating the option of doubling the frequency to obtain light in the green at 532 nm. Because of the higher energy per photon in the green only half the power is required to reach the same shot-noise limited sensitivity. Also the optical components can be smaller because the diffraction-limited beam-diameter is smaller in the green by the square-root of two. Doubling efficiencies around 50 percent have been achieved by others for powers around 10 W and much more seems possible [18]. This option will be investigated over the next two years.

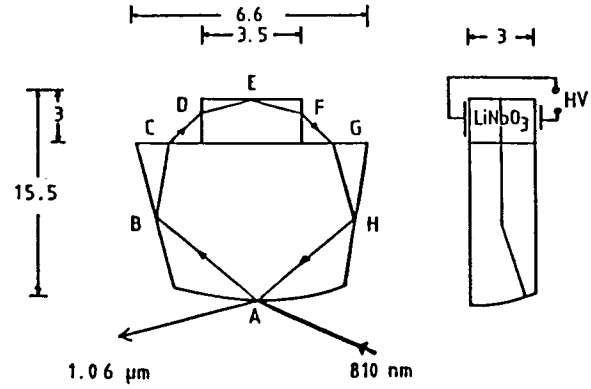

Fig. 4. Monolithic Nd-YAG ringlaser (dimensions in mm)

3.1.2 Frequency Noise

A perfect interferometer is entirely insensitive to frequency fluctuations of the laser. But in a real interferometer, noise signals can be created if at the output of the interferometer there is interference of lightbeams that have a different history. Such a situation can arise if the storage times in the

arms are not identical, or if stray light can reach the output through a path different from that of the main beam. If the relative amplitude of stray light capable of interfering with the main beam is σ, then the arm-length change $\frac{\delta\ell}{\ell}$ simulated by a frequency change $\frac{\delta\nu}{\nu}$ of the laser is

$$\frac{\delta\ell}{\ell} = \sigma\frac{\delta\nu}{\nu}, \tag{2}$$

if stray-light with a path-difference of one full round-trip dominates.

The prototypes use relatively noisy Argon lasers that require sophisticated frequency stabilization techniques. Figure 5 shows as an example the unstabilized frequency noise of the laser previously used on the Garching prototype, curve (a). Curve (b) shows the noise after prestabilization onto a rigid Fabry-Perot reference resonator, and curve (c) shows the noise after final stabilization onto the average armlength of the 30-m interferometer. A lowest value of about $5 \times 10^{-3}\mathrm{Hz}/\sqrt{\mathrm{Hz}}$ is reached in the relevant frequency range. The Argon laser in the Glasgow prototype, being stabilized onto the 10 m long Fabry-Perot cavity in one of the interferometer arms using similar techniques, reaches a frequency noise of a few times $10^{-5}\mathrm{Hz}/\sqrt{\mathrm{Hz}}$.

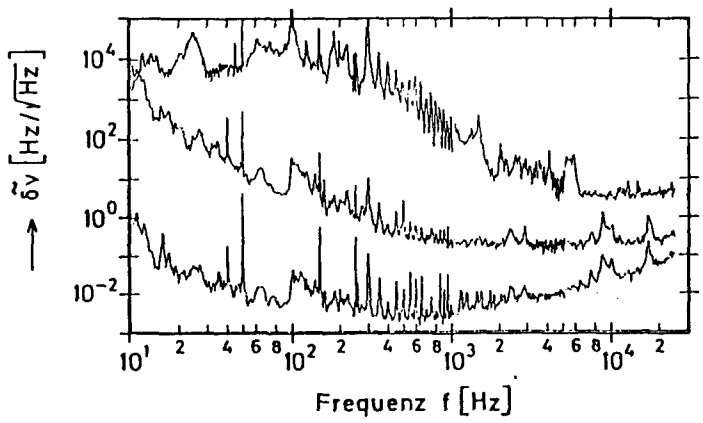

Fig. 5. Frequency noise of the Garching Innova 90-5 laser:
(a) upper curve: unstabilized laser,
(b) middle curve: laser stabilized onto a 25-cm rigid Fabry-Perot,
(c) lower curve: laser stabilized onto the interferometer armlength.

For a full-scale detector, the frequency-noise out of the laser must be smaller than $10^{-6}\mathrm{Hz}/\sqrt{\mathrm{Hz}}$. But for the diode-pumped YAG laser the unstabilized frequency noise is orders of magnitude smaller than for an Argon laser. So achieving the same gain in the feed-back loop as for the Argon laser is already enough to reach the desired stability goal.

3.2 Recycling

Clearly the sensitivity of a simple Michelson interferometer is not sufficient, even if very strong lasers are used. Two techniques have been developed that improve the interferometer sensitivity to a level that would allow the detection of gravitational wave signals with high confidence. These techniques are known as Power Recycling and Signal Recycling, and the combination of both as Dual Recycling [13].

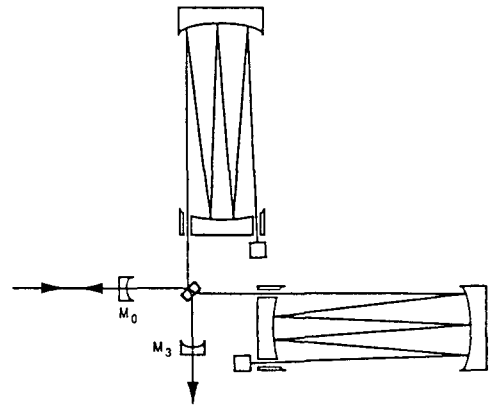

Fig. 6. Dual recycled interferometer

Power Recycling makes use of the fact that the interferometer output is held on a dark fringe by a feed-back loop and almost all the light goes back towards the input, i.e. the locked interferometer behaves as a mirror. By placing a mirror in the input of the interferometer, a resonant optical cavity can be formed that uses the whole locked interferometer as an end mirror. So the circulating light power inside the interferometer will be higher than the laser power by the inverse of the losses in the interferometer.

Signal Recycling works similarly, except that it leads to a resonant enhancement of the signal instead of the light. A gravity wave shaking the mirrors will phase modulate the reflected laser light, or in other words create side-bands of the laser frequency. These side-bands exit through the output port of the interferometer. By placing another mirror there, a resonant cavity for the signal-containing side-bands is formed. Depending on the reflectivity of this mirror, the detector can be made to operate narrow-band or broad-band, and by changing the position of this mirror the interferometer can be tuned. As an additional advantage, this configuration greatly reduces the power losses due to bad interference, because the light can no longer escape the interferometer through the output port, which is now closed by the signal recycling mirror. Just as the signal recycling cavity enhances light at its resonant mode and frequency, it suppresses light

which, through aberrations, got diffracted into non-resonant modes of the light field.

The shot noise-limited sensitivity of a Dual Recycled interferometer to gravitational wave bursts is given by

$$h_{\mathrm{DL}} \approx 10^{-22} \left[\frac{f}{1\,\mathrm{kHz}}\right] \left[\frac{\epsilon I_o}{50\,\mathrm{W}}\right]^{-1/2} \left[\frac{1-R}{5\times 10^{-5}}\right]^{1/2} \left[\frac{\ell}{3\,\mathrm{km}}\right]^{-1/2}, \quad (2)$$

where f is the center frequency of the burst, ϵ is the quantum efficiency of the detector, I_o is the laser output power, ℓ is the arm-length, and R is the mirror reflectivity. Green light and a bandwidth of half the center frequency have been assumed.

3.3 Mirror Losses

In order to make these recycling techniques work, we need mirrors with extremely small losses. This requires substrates with a microroughness on the order of an Angstrom and reflective coatings with very small scatter and absorption. Fortunately, the last few years have brought us tremendous advances in the art of making superpolishes and supercoatings. Mirrors with reflection losses of much less than 50 parts per million are now available from several sources.

But it is not just the linear reflection losses that are responsible for the total losses in the Power Recycling cavity. One of the "mirrors" of this cavity is actually a very complicated object, - an interferometer locked to a dark fringe. So any effect that degrades the interfering wavefronts will let light leak out the wrong port of the interferometer. Though some of this light can be recovered by the Signal Recycling mirror, this is a serious loss process for the Power Recycling cavity.

There are two main reasons for a degradation of the interference in the interferometer: wavefront deformation because of imperfections of optical elements and because of thermal effects in the optical elements. Both processes can be addressed through optical modeling and numerical wavefront propagation calculations.

3.3.1 Thermal Distortions

Thermal effects can arise because of absorption in the optical coatings or in the bulk of elements used in transmission. This will cause a deformation of the substrates and/or a lensing effect through thermally induced refractive index changes. Figure 7 is the result of a model calculation including thermal effects for the main mirrors [19]. It shows the interference minimum as a function of the thermally induced mirror deformation. For increasing light power, the interference quality deteriorates in a very non-linear fashion, even approaching chaotic looking behaviour above a certain threshold.

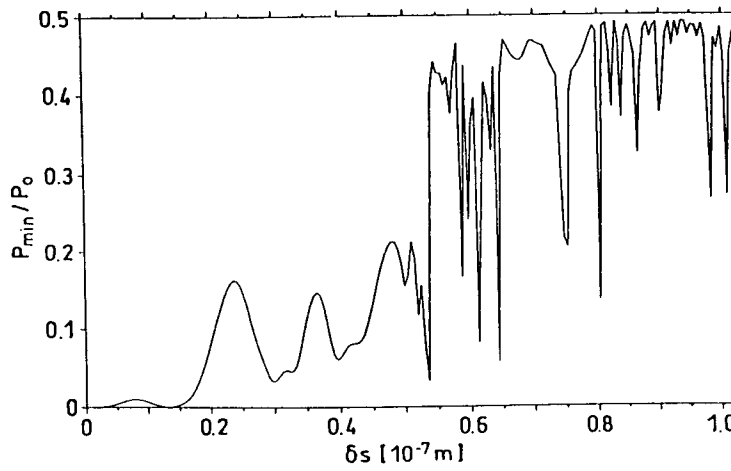

Fig. 7. Power loss due to thermal effects:
interference minimum as a function of local mirror deformation.

We have studied the absorption in coatings produced in ion beam sputtering chambers (one of which we have access to inside the collaboration at LZH). Fortunately, the absorption in modern coatings is only on the order of very few parts per million and thermal effects seem very tractable. Absorption in the bulk of the beam-splitter will probably be the limiting process at circulating powers of many kilowatts.

3.3.2 Mirror Quality

Existing supermirrors with almost negligible losses have been developed for applications using spot sizes of a millimeter or so. For large laser interferometers the beam size will be on the order of several centimeters and the high demands on the surface quality now extend to much larger lateral dimensions. Surface deformations on length scales of several centimeters will behave just as the microroughness does for the smaller beams. But it is not the substrate alone that determines the surface quality. The reflective dielectric multilayer stack coated onto the mirror can show variations of its effective thickness that may overwhelm the surface variations of the substrate.

3.3.3 Optical Modeling

Using a numerical wavefront-propagation code running on the Garching Cray Y-MP, we are studying the effects of surface deformations on the light fields in the interferometer. Currently this code can propagate optical wavefronts on a 4000 x 4000 grid. So it is possible to even include scattering

to angles large enough for the light to miss the end mirror entirely and to hit the vacuum tube after a few hundred meters. This light will then be converted into the diffuse background of scattered light. The code takes as its input assumed or measured surface profiles of the relevant mirrors. Surface deviations from the ideal shape can be measured with today's state-of-the-art to an accuracy of a few Angstroms over a field of a quarter of a meter with a lateral resolution of half a millimeter [20].

As an example, Fig. 8 shows the output field expected for a 3-km interferometer with a mirror distortion of $\lambda/1000$ amplitude on a length scale equal to the beam diameter. The code permits us to simulate all kinds of mirror distortions and to predict the performance of a specific mirror in practice. Through an R+D contract with Zeiss we are addressing the mirror manufacturing problem and we are confident that in 1992 the first prototype mirrors with the required quality will be finished.

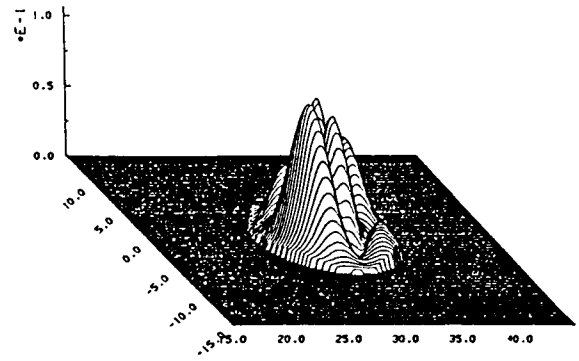

Fig. 8. Output field for mirror with $\lambda/1000$ distortion

3.4 Thermal Noise

3.4.1 Mirror Internal Noise

The mirrors are macroscopic objects and, correspondingly, have internal mechanical vibration modes. Even for perfectly well isolated mirrors, these resonances will still get thermally excited. At the resonant frequencies the mechanical vibration amplitudes are too large and will overwhelm any mirror motion due to a possible gravitational wave. The only solution is to shift all mechanical resonances out of the frequency range of interest by a suitable choice of mirror shape and material. The best compromise is obtained for cylindrical mirrors with a length about half the diameter. For synthetic quartz this yields resonant frequencies of a few kHz, - above the interesting frequency window.

But even though the resonances are outside the observation window, the *sub-resonant wings of those resonances do cause a stochastic motion of the* mirror surface. The strain spectral density due to these motions is given by

$$\tilde{h} \approx \sqrt{\frac{16kT}{\pi^3 \rho {v_s}^3 Q_{\mathrm{INT}} \ell^2}}, \tag{3}$$

where ρ is the density, ℓ the arm-length, v_s the sound velocity, and Q_{INT} the mechanical quality factor of the mirror material. Note that this expression is independent of mirror size. It is mandatory to use a material with very low internal damping (very high Q). Single crystal Silicon suggests itself for the non-transmitting components with a Q of up to 10^8, but even synthetic quartz gives a Q of a few hundred thousand, whereas low-expansion Zerodur only has a Q of about 1000. Special attention has to be paid to the way of suspending the mirrors, because any way of dissipating energy, like friction of a rubbing suspension wire, will immediately destroy an internal Q as high as this. The problem of material Q as a function of experimental parameters is currently being investigated by us [21].

It should be noted that the noise density due to thermal mirror noise will be strictly constant in frequency only if the internal damping mechanism has viscosity-like behaviour. Sub-resonant thermal noise like this has never been measured directly, but it is highly likely that the mechanical mirror resonance will behave much more like a harmonic oscillator with a complex spring constant [22]. In this case the thermal noise would actually increase from the quoted level towards lower frequencies like the inverse of the square-root of the frequency.

3.4.2 Suspension Noise

Thermal noise is also present in the last stage of the vibration isolation system. This will be a simple wire pendulum made from a sling supporting the mirror. In this case the resonant frequency is about 1 Hz, and the frequency window of observation is on the above-resonant wing. The spectral density of apparent strain noise due to this effect is given by

$$\tilde{h} \approx \sqrt{\frac{16kT\omega_o}{mQ_S\omega^4\ell^2}}, \tag{4}$$

where m is the mirror mass, ω_o the resonant frequency and Q_S the mechanical quality factor of the suspension pendulum. This Q can be much higher than the internal Q of the wire material because most of the energy of the pendulum is in the form of potential and kinetic energy of the swinging bob and not in the elastic energy of a bent wire. But it is extremely important that the wire support points be properly designed to avoid friction. Pendulum Qs as high as 10^7 have been experimentally observed [25],

(meaning that a 1 Hz pendulum will oscillate for more than 4 months before its amplitude has decreased to one-third).

3.5 Vibration Isolation

We are trying to measure very small length changes due to the action of gravitational waves and so it is extremely important to ensure that no other effect moves the test masses. By far the largest disturbance is the random ground motion because of the natural seismic activity. The spectral density of displacement due to seismic ground motion typically falls of as

$$\tilde{x}(f) \approx 10^{-7}\mathrm{m}/\sqrt{\mathrm{Hz}}\left[\frac{1\mathrm{Hz}}{f}\right]^2 . \tag{5}$$

At a frequency of 1 kHz, this is about 10^7 times larger than the effect we are trying to measure and we require an effective way of vibration isolating the test masses.

Passive vibration isolation is, in principle, straightforward [23]. The object to be isolated gets suspended by a pendulum. If a disturbance shakes the suspension point of the pendulum with a frequency below its resonant frequency, then the pendulum will transmit the disturbance unattenuated. But a disturbance above the resonant frequency f_o will get attenuated with the ratio $(f_o/f)^2$ up to a frequency Qf_o, where the frequency dependence changes to a linear slope. The resonant frequency f_o should thus be as low as possible. Due to practical limitations on the pendulum length to around one meter, horizontal resonant frequencies are usually limited to around 1 Hz. Vertical resonant frequencies are normally a bit higher because the spring has to be stiff enough to support the full load. Several of these stages can be cascaded to achieve a very steep fall-off above the highest normal mode of the coupled oscillator system.

3.5.1 Stacks

A very simple, yet very effective way of achieving vibration isolation at moderately high frequencies (above 100 Hz) is the use of vibration isolation stacks. A detailed analysis of stack systems has recently been carried out by Cantley et al [26]. Stacks are basically alternating layers of a high-density material (like lead) and rubber. Each layer acts as a 3-dimensional pendulum, although with a fairly low Q. But since it is easy to use several such layers, a rather steep fall-off towards higher frequencies can be achieved. As an example, Fig. 9 shows a comparison between calculated and measured transmissibility of a small 4-layer lead-rubber stack intended for the Garching prototype.

Because of their low mechanical Q-factor, such stacks show a rather high thermal noise. The last two stages of the suspension should accordingly be very high-Q wire pendulums of low resonant frequency. These will

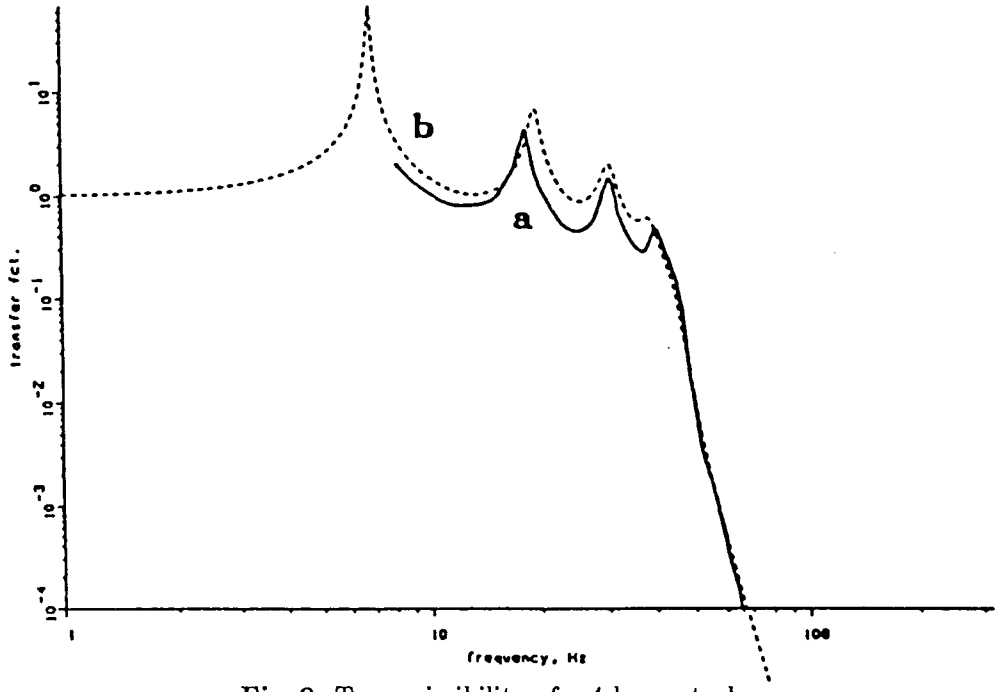

Fig. 9. Transmissibility of a 4-layer stack

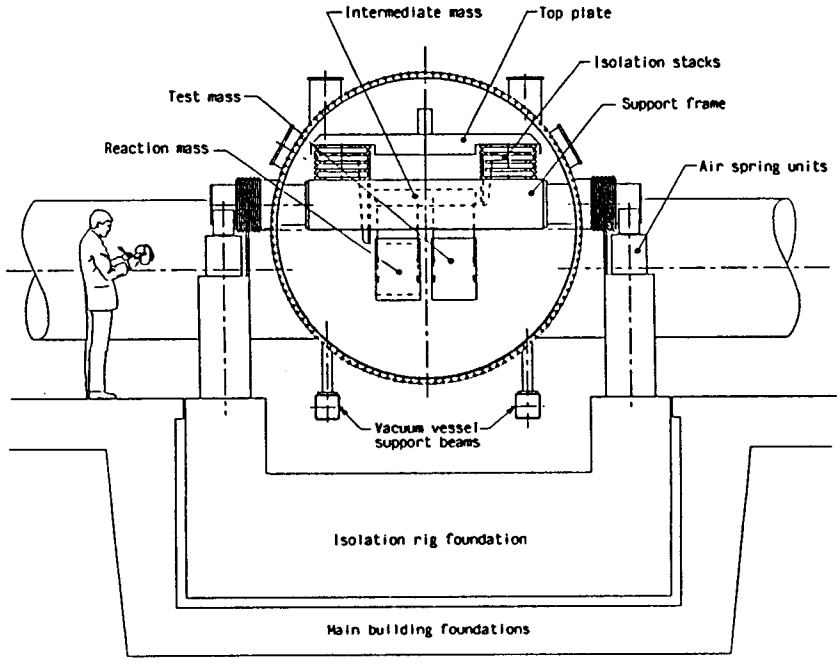

Fig. 10. GEO suspension

also give an additional $1/f^4$ filtering in the horizontal direction where it is most critical (this is the direction of the laser beam; in principle, vibration isolation in the vertical direction is only required because of the unavoidable cross-coupling between the two degrees of freedom).

The design chosen for the GEO suspension is shown in Figs. 10 and 11. It consists of an active airspring system as a first stage to give some very low-frequency isolation. Supported by this system is a five-layer isolation stack supporting the top plate. Each of the layers has a horizontal resonant frequency of 10 Hz, a vertical resonance at 30 Hz and a Q of about 2. The top plate is a hollow structure filled with damping material to suppress structural resonances. The mirror is suspended from the top plate through a double wire pendulum with an intermediate mass. Each of these pendulums has a resonance at 1 Hz. Some small components that require fast feedback (see below) are paired up with reaction masses. The total isolation as expected from model calculations should be more than sufficient at all frequencies above 100 Hz.

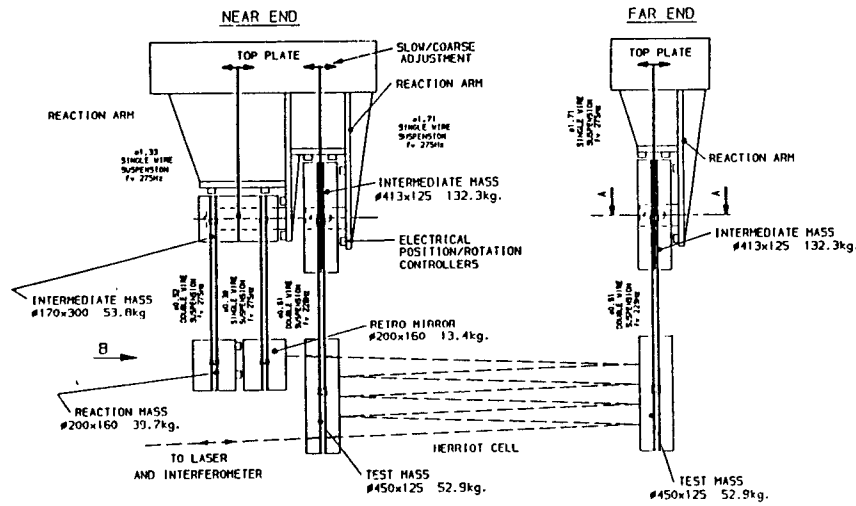

Fig. 11. GEO suspension

3.5.2 Low-Frequency Isolation

Extending vibration isolation down to lower frequencies becomes increasingly difficult. The ground noise spectrum increases towards lower frequencies like $1/f^2$ and the isolation decreases because one is moving closer to the highest normal mode of the pendulum chain. Some very promising work on low frequency passive isolation has been done in Pisa [34]. The 12 m-high Superattenuator uses a cascade of an inverted pendulum, 7 gas springs, and

a wire pendulum to achieve efficient vibration isolation above 10 Hz. If the control problems associated with this approach can be solved, it could be an alternative to the use of stacks.

Another way of achieving isolation at very low frequencies would be the use of active or combined active/passive vibration isolation systems. Some very promising work, aiming at achieving isolation all the way down to 1 Hz, is going on at the Joint Institute for Laboratory Astrophysics in Boulder, Colorado [28].

3.6 Position Control and Feed-Back

An interferometer with as many components and degrees of freedom as a gravitational wave detector requires sophisticated control systems to keep all parameters at their optimal operating points. The guiding principle behind the position control of the optical components is easily stated: At low frequencies the optical components must be rigidly held relative to each other to keep them from drifting and to prevent the interferometer and the recycling cavities from losing lock. On the other hand, at higher frequencies, where gravitational wave signals could be detected (above 100 Hz), the test masses must be totally free and the system used to prevent them from moving at low frequencies must not exert any residual forces at high frequencies. Three main classes of control systems are used:

3.6.1 Local Controls

The suspension of the optical components via high-Q pendulums is an efficient way to isolate them from high-frequency vibrations and pendulum thermal noise. But at the resonant frequencies of the undamped suspension, large vibration amplitudes can occur that will greatly exceed the dynamic range of the detector (a pendulum with a Q of 10^7 can, at its resonance, lead to an amplification of up to 10^7). The resonance must thus be damped. But damping it in the usual dissipative way will degrade the Q and introduce thermal noise. The damping is instead done in an active and frequency-selective way. This technique is routinely used on the prototypes. The position of the masses is sensed with a low-noise local sensor. This signal is then electronically filtered to a narrow frequency range around the resonance and then fed back to a force transducer acting on the mass selectively in this band around the resonant frequency only. On the prototypes the position sensing is usually done via shadow sensors consisting of a LED-photodetector pair with the light path partly interrupted by a movable vane mounted on the test mass. The force is applied through a coil acting on a magnet on the mass. Such systems typically show a sensing noise of around $10^{-11}\mathrm{m}/\sqrt{\mathrm{Hz}}$. In the full scale detector we are trying to measure displacements smaller than $10^{-20}\mathrm{m}/\sqrt{\mathrm{Hz}}$. So the servo gain would have to roll off by

9 orders of magnitude in the small frequency range from a few Hz to 100 Hz, which is clearly a formidable task. The problem can be solved by sensing the motion of, and applying feed-back to, a higher stage in the suspension system and using the passive $1/f^2$ filtering of each stage. Such systems are currently being tested in the prototypes.

3.6.2 Global Controls

In order to optimally align an optical interferometer, and keep it aligned regardless of drift or stability of the optical components, some kind of automatic alignment system is required. The guiding principle is that the alignment signals for such a system should be derived directly from the existing interfering beams without introducing additional components into the high-sensitivity/high-intensity part of the interferometer. Suitable feed-back should then be applied to all the relevant optical components.

For example, consider the case of two interfering beams, where a differential high frequency phase modulation is applied and the overall phase difference is determined by coherently demodulating the intensity of the interfered output. Relative angular misalignment introduces a differential phase gradient between the two beams which can be sensed using a split photodiode and coherently demodulating as before. Lateral misalignment may be detected using another split photodiode and a suitable lens arrangement to cause laterally offset beams to converge.

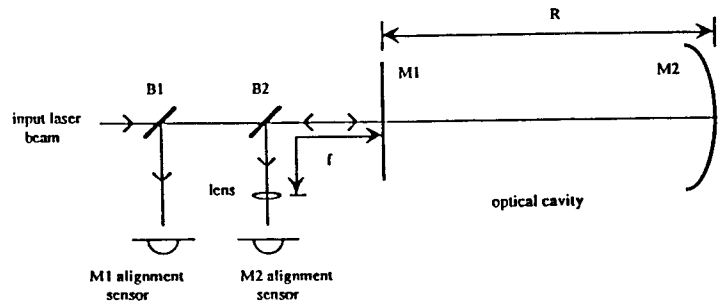

Fig. 12. Automatic alignment of a Fabry-Perot cavity

An illustration of this techniques for a Fabry-Perot cavity is given in Fig. 12. All 4 degrees of freedom necessary for alignment can be extracted. An extension of this technique can be used to automatically align all degrees of freedom for all components of the interferometer. A system similar to the automatic alignment system intended for the large interferometer is being

installed and tested in the Glasgow prototype [27] and will be installed in the Garching prototype after it is reconstructed.

3.6.3 Fast Feed-Back

While high-frequency ground motions can be efficiently suppressed by the suspension system, there are very-low frequency seismic motions (1 Hz and less) that are very difficult to isolate against. This very-low frequency seismic motion may lead to rms differential arm-length changes of several microns. Unsuppressed, these would lead to a severe limitation of the sensitivity of the detector, because an interferometer operating away from its null fringe by an amount δx becomes sensitive to the intensity fluctuations δI of the laser according to

$$h_{\text{noise}} = \frac{\delta x}{\ell} \frac{\delta I}{I} \tag{6}$$

The sensing in this case is no problem, because the main interferometer output itself provides the signal. But these deviations from the null have to be suppressed by at least 10^6 which requires a fast servo with a bandwidth of order a kHz. These correction signals will be applied to the small optical components in the 3-km interferometer such as beam-splitter and retro-mirror. This feed-back is best applied relative to a reaction mass suspended from the same isolation system to avoid coupling ground motion back in through the actuator (see Fig. 11).

3.7 Vacuum System

At the required sensitivity, the whole detector must operate in a high vacuum to reduce noise from gas molecules. The limiting criterion is the fluctuation in the refractive index due to changes in the average density of the gas through which the laser beams pass, resulting in phase shifts of the interfering light beams. If these changes occur in the frequency window of observation (from a few tens of Hz to a few kHz) they can mask gravitational events.

Pressure fluctuations can arise from the random motion of the gas molecules in the vacuum tubes and chambers. The amplitude of a fluctuation is proportional to the square root of the pressure. To reach the proposed sensitivity of the detector, a pressure smaller than 10^{-8}mbar is required for Hydrogen. Since other gases have higher refractive indices, the sum of their partial pressures should be smaller than 10^{-9}mbar. Finally, the system should be hydrocarbon free as far as technically possible.

Pressure fluctuations can also arise from changes in the pumping speed. There are mechanisms which could cause fluctuations in pumping speed for most UHV pumps. Ion pumps have noisy discharge currents, cryogenic pumps are likely to emit bursts of gas and even turbomolecular pumps can

show variations of their pumping speed due to asymmetries and fluctuations in the rotation or variations in the backing line. We are currently investigating the subject of fast pressure bursts due to vacuum pumps.

However, it is difficult to think of mechanisms for fluctuations in the pumping speed of non-evaporable getter (NEG) pumps. Also, their operation is completely vibration-free. As a result, 21 NEG pumps of 14 000 l/s capacity each have been chosen in our conceptual design to provide the main UHV pumping [24].

The vacuum tubing carrying the laser beams up and down the two arms will have a total length of 6 km and a diameter of 1.4 m and will be one of the largest UHV systems in the world. It will be one of the most costly elements of the detector. It is thus worthwhile to look for unconventional designs to save costs on this component. We are proposing to use a thin-walled (0.7 mm) tube made from 316L stainless steel sheet material. To provide stability, it would have a continuous corrugation with a height of 40 mm peak-to-peak over the whole length of the tube. Such a tube, if continuously manufactured and welded on site, would cost only a small fraction of a more traditional thick-walled and flanged tube. Vacuum tests on a 5 m-long test section showed very promising results, especially a very low outgassing rate of 3×10^{-13} mbar l/s/cm^2 after baking it at only 150 C [24].

Before deciding on this design for the final detector, more tests have to be done on a much longer test section manufactured under field conditions. These tests are currently being prepared by the European research groups.

4 Detector Realization

The proposed detector consists of two perpendicular arms, each of 3 km length. The vacuum system is designed to accommodate two simultaneously operating interferometers which can be optimized to different parameters. Commissioning is planned to proceed in steps from a simple Michelson interferometer to a full Dual-Recycled system and will take several years after the installation of the first interferometer. After reaching a burst sensitivity of 10^{-21} we expect to split the available detector time roughly equally between observation runs and experimental work to push the sensitivity further towards a value of 10^{-22}. The significance of the various noise sources for the sensitivity of a fully optimized interferometer to broad-band gravitational wave bursts is shown in Fig. 13. The curve labeled seismic noise is valid for the described stack system. With a Pisa-type suspension, the curve would be moved to the left edge of the figure and the low-frequency sensitivity would be limited by thermal suspension noise. The thermal noise in Fig. 13 has been calculated assuming viscosity-like internal damping for mirrors and suspension.

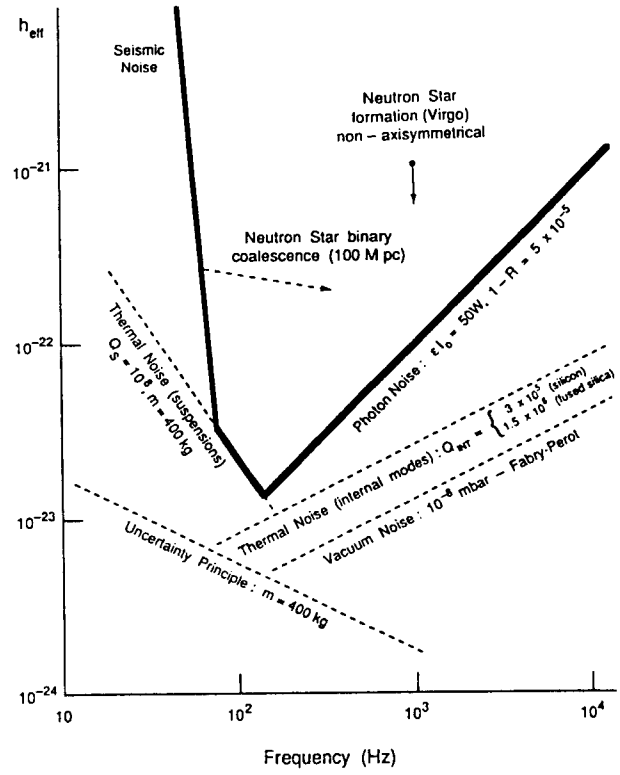

Fig. 13. Noise sources relevant for the detector

The site selection survey was finished in 1991 and two suitable sites were identified near Hannover in the German state of Niedersachsen. One of them is a flat, dry and uninhabited piece of land owned by the state government. Here, the tunnel housing would be a concrete structure with 3 m internal height and a width of 4 m submerged in a trench close to the surface. The control building as well as the laboratory buildings containing the vacuum tanks and the optics would be conventional structures above ground. The other possible site is a mountain site also owned by the state government. Here, the arms would be in a 4-m diameter underground tunnel cut through bedrock. The vacuum tanks and optics at the vertex and the ends of the arms would be in 35-m diameter underground caverns, but each of the three corner caverns would be accessible from the outside through short horizontal access tunnels. Only the control building would be visible above ground. Geological, hydrological and seismological investigations found both sites very suitable; the mountain site having an advantage with respect to seismic noise, of course. Costings and architectural designs have been prepared. Construction at the underground site has been found to be more expensive

by about 15 percent. The final decision between the two sites will be made in 1992, largely based on necessary additional environmental impact studies. An impression of the main control building is given in Fig. 14.

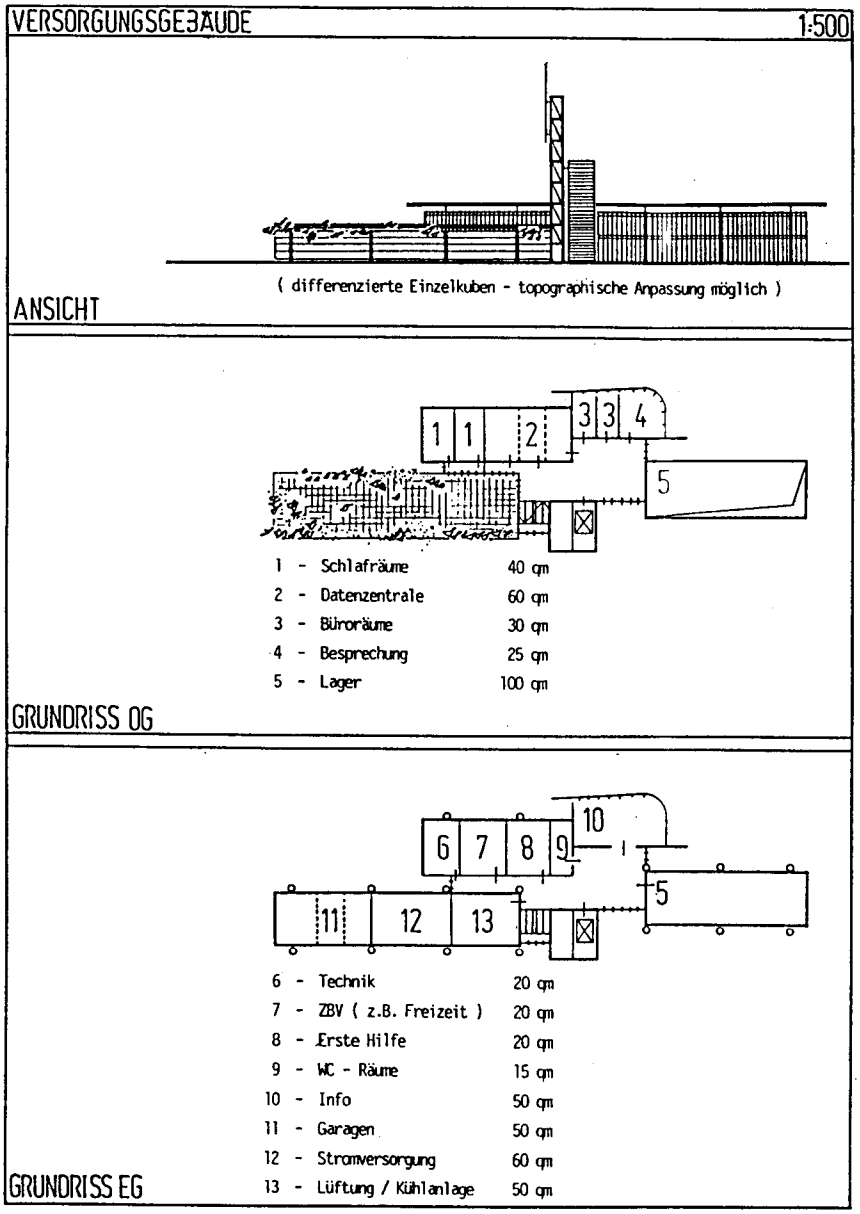

Fig. 14. GEO main building

5 Status of Efforts in the World

5.1 Proposals

The American LIGO proposal [29] calls for the construction of two detectors with 4 km arm-length. It was approved in the fall of 1991 and funds have been appropriated by Congress. Two sites were selected in the spring of 1992, one in Hanford, Washington and the other in Livingston, Louisiana. Construction is expected to begin in 1993 and commissioning may start as early as 1997.

An Australian proposal (AIGO) for a 3-km detector [30] has been submitted, but has not been able to obtain approval.

In Japan, a proposal for an intermediate 100-m interferometer (TENKO-100) [31] has been funded. Construction may be finished in 1994. In parallel, plans are being developed for a 3-km interferometer.

The French-Italian VIRGO collaboration [32] has proposed a 3-km interferometer to be built near Pisa and the German-British GEO collaboration [15] has proposed a 3-km interferometer to be built near Hannover. Both interferometers are being coordinated under the EUROGRAV framework. A decision from all the relevant governments in Europe is expected in the summer of 1992.

5.2 A World-Wide Network

All these projects are not in competition with each other. On the contrary, each of the projects is crucially dependent on the others. To sort out gravitational wave events from the ever-present noise background requires observation in coincidence of several detectors. So two gravitational wave detectors are the absolute minimum to even prove the existence of gravitational waves. But to fully unravel the information contained in the signals with respect to the source direction, time structure and polarization requires a world-wide network of four detectors [33].

If all goes well, this network can be in place by the end of this decade, and at the beginning of the next millenium we may be able to mark the beginning of the age of Gravitational Astronomy.

References

1. C.W. Misner, K.S. Thorne, and J.A. Wheeler, *Gravitation* (Freeman, San Francisco, 1973).
2. J.H. Taylor and J.M. Weisberg, Astrophys. J. **345**, 434 (1989).
3. K.S. Thorne in *Gravitational Radiation*, edited by N. Deruelle and T. Piran (North Holland, Dordrecht, 1983), pp. 1-54.
4. K.S. Thorne in *Recent Advances in General Relativity*, edited by A. Janis and J. Porter (Birkhauser, Boston, 1992), pp. 196-229.

5. J. Weber, Phys. Rev. **117**, 306 (1960).
6. P.F. Michelson, J.C. Price, R.C. Taber, Science **237**, 150 (1987).
7. F.A.E. Pirani, Acta Physica Polonica **15**, 389 (1956).
8. M.E. Gertsenshtein and V.I. Pustovoit, JETP **16**, 433 (1963).
9. R. Weiss, Quarterly Progress Report of RLE, MIT **105**, 54 (1972).
10. G.E. Moss, L.R. Miller, R.L. Forward, Applied Optics **10**, 2495 (1971).
11. R.W.P. Drever in *The Detection of Gravitational Waves*, edited by D. Blair (Cambridge University Press, Cambridge, 1990), pp. 306-328.
12. W. Winkler, ibid.
13. B.J. Meers, Phys. Rev. D **38**, 2317 (1988); K.A. Strain and B.J. Meers, Phys. Rev. Lett. **66**, 1391 (1991).
14. D. Shoemaker, R. Schilling, L. Schnupp, W. Winkler, K. Maischberger and A. Rüdiger, Phys. Rev. D **38**, 423 (1988); T.M. Niebauer, R. Schilling, K. Danzmann, A. Rüdiger, and W. Winkler, Phys. Rev. A **43**, 5022 (1991).
15. J. Hough et al., *Poposal for a Joint German-British Interferometric Gravitational Wave Detector*, Max-Planck-Institut für Quantenoptik, Report No. MPQ 147 (1989), unpublished.
16. G.A. Kerr and J. Hough, Appl.Phys. B **49**, 491 (1989).
17. I. Schütz, H. Welling and R. Wallenstein, in *Advanced Solid State Lasers* (Salt Lake City, 1990).
18. R.L. Byer, private communication.
19. W. Winkler, K. Danzmann, A. Rüdiger, and R. Schilling, Phys. Rev. A **44**, 7022 (1991).
20. K. Freischlad, M. Küchel, W. Wiedmann, W. Kaiser, and M. Mayer, Proc. SPIE **1332**, 8 (1990).
21. J.E. Logan, N.A. Robertson, J. Hough, and P.J. Veitch, Phys. Lett. A **161**, 101 (1991).
22. P.R. Saulson, Phys. Rev. D **42**, 2437 (1991).
23. N.A. Robertson in *The Detection of Gravitational Waves*, edited by D. Blair (Cambridge University Press, Cambridge, 1990).
24. J.R.J. Bennett and R.J. Elsey, Vacuum **43**, 35 (1992).
25. W. Martin, Ph.D. Thesis, Glasgow (1978), unpublished.
26. C. Cantley et al., Rev. Sci. Instr. **63**, 2210 (1992).
27. E. Morrison et al., to be published.
28. P.G. Nelson, Rev. Sci. Instr. **62**, 2069, 1991.
29. R.E. Vogt, R.W. Drever, F.J. Raab, K.S. Thorne, and R. Weiss, *Laser Interferometer Gravitational-Wave Observatory*, proposal to the National Science Foundation, (California Institute of Technology, December 1989), unpublished; A. Abramovici et al., Science (1992), in press.
30. R.J. Sandeman, D.G. Blair, and J. Collett, *Australian International Gravitational Research Centre*, proposal to the CRC, (Australian National University, 1991), unpublished; D.E. McClelland et al. in *Gravitational Astronomy*, edited by D.E. McClelland and H.A. Bachor (World Scientific, Singapore, 1991).
31. N. Kawashima in *Gravitational Astronomy*, edited by D.E. McClelland and H.A. Bachor (World Scientific, Singapore, 1991); M. Fujimoto, M. Ohashi, N. Mio, and K. Tsubono, ibid.

32. C. Bradascia et al. in *Gravitational Astronomy*, edited by D.E. McClelland and H.A. Bachor (World Scientific, Singapore, 1991).
33. Y. Gürsel and M. Tinto, Phys. Rev. D **40**, 3884 (1990).
34. R. DelFabbro et al., Rev. Sci. Instr. **59**, 292 (1988); C. Bradascia et al., Phys. Lett. A **137**, 329 (1989).